Modeling Dye–Sensitized Solar Cells: From Theory to Experiment

ARTICLE *in* JOURNAL OF PHYSICAL CHEMISTRY LETTERS · MARCH 2013

Impact Factor: 7.46 · DOI: 10.1021/jz400046p

6 AUTHORS, INCLUDING:

Tangui Le Bahers
Claude Bernard University Lyon 1
33 PUBLICATIONS **856** CITATIONS
SEE PROFILE

Thierry Pauporté
Chimie ParisTech
163 PUBLICATIONS **4,724** CITATIONS
SEE PROFILE

Philippe P Lainé
Paris Diderot University
46 PUBLICATIONS **1,320** CITATIONS
SEE PROFILE

THE JOURNAL OF PHYSICAL CHEMISTRY Letters

Perspective

pubs.acs.org/JPCL

Modeling Dye-Sensitized Solar Cells: From Theory to Experiment

Tangui Le Bahers,*[,†] Thierry Pauporté,[‡] Philippe P. Lainé,[§] Frédéric Labat,[‡] Carlo Adamo,*[,‡,∥] and Ilaria Ciofini*[,‡]

[†]Université Claude Bernard Lyon 1, Ecole Normale Supérieure de Lyon, Laboratoire de Chimie, 46 Allée d'Italie 69364 Lyon Cedex 07, France

[‡]LECIME, Laboratoire d'Electrochimie, Chimie des Interfaces et Modélisation pour l'Energie, UMR 7575 CNRS, Ecole Nationale Supérieure de Chimie de Paris − Chimie ParisTech, 11 rue P. et M. Curie, 75231 Paris Cedex 05, France

[§]Université Paris Diderot, Sorbonne Paris Cité, ITODYS, UMR 7086 CNRS, 15 rue Jean-Antoine de Baïf, 75013 Paris, France

[∥]Institut Universitaire de France, 103 Boulevard Saint Michel, F-75005 Paris, France

Supporting Information

ABSTRACT: Density functional theory (DFT) and time-dependent DFT are useful computational approaches frequently used in the dye-sensitized solar cell (DSSC) community in order to analyze experimental results and to clarify the elementary processes involved in the working principles of these devices. Indeed, despite these significant contributions, these methods can provide insights that go well beyond a purely descriptive aim, especially when suitable computational approaches and methodologies for interpreting and validating the computational outcomes are developed. In the present contribution, the possibility of using recently developed computational approaches to design and interpret the macroscopic behavior of DSSCs is exemplified by the study of the performances of three new TiO_2-based DSSCs making use of organic dyes, all belonging to the expanded pyridinium family.

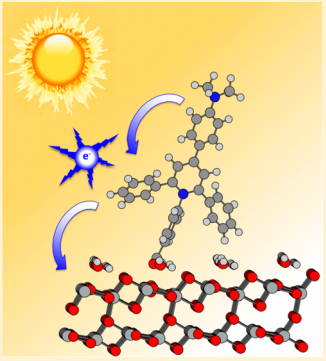

In 1991, when the first dye-sensitized solar cell (DSSC) was completely characterized by Grätzel and O'Regan,[1] DSSC photovoltaic technology completely broke out of conventional principles of photovoltaic devices by multiplying the interfaces and the chemical nature of each component. Grätzel and O'Regan showed that if the electron transfer mechanism at each interface is optimized, then the final photoconversion efficiency can be, at least in principle, as high as in standard photovoltaic devices. From that moment, the interest of the scientific community for this technology has never ceased to grow.

In DSSCs, light is harvested by dye molecules grafted on a large surface and wide bandgap semiconductor (such as TiO_2 or ZnO) in contact with an electrolyte containing a redox pair as a charge mediator (M/M^{ox}), while the circuit is closed by a counter electrode, usually made of platinum, Pt.

$$\mathrm{Dye} + h\nu \rightarrow \mathrm{Dye}^* \quad (1)$$

$$\mathrm{Dye}^* \rightarrow \mathrm{Dye}^+ + e^-_{n-SC} \quad (2)$$

$$\mathrm{Dye}^+ + M \rightarrow \mathrm{Dye} + M^{ox} \quad (3)$$

$$M^{ox} + e^-_{Pt} \rightarrow M \quad (4)$$

Upon absorption of light, dye molecules are promoted in an electronically excited state (eq 1), which normally lies above the bottom edge of the semiconductor conduction band so that injection of electrons into this latter is thermodynamically favorable (eq 2). Oxidized dyes are regenerated in their native state by a reducing agent present in the electrolyte (the mediator M), which is consequently converted to the corresponding oxidized species (M^{ox}, eq 3). The latter, after diffusion in the electrolyte, is reduced at the counter-electrode (e.g., Pt; eq 4). The overall charge carriers' motion gives rise to the macroscopic photocurrent, while the photoinduced electron transfer from the dye to the semiconductor, increasing the electronic density in the oxide, gives rise to an electrochemical potential difference (i.e., a voltage) between the semiconductor and the electrolyte.

The overall photoconversion efficiency, η, is thus defined as follows:

$$\eta = \frac{V_{oc} J_{sc} \mathrm{FF}}{P_i} \quad (5)$$

where J_{sc} is the photocurrent density at short-circuit, V_{oc} is the open-circuit photovoltage, P_i is the power of the incident light, and FF is the fill factor. This latter defines the ratio of the actual maximum obtainable power to the product of the open circuit voltage and short circuit current.

Two decades have passed since the first DSSC characteristics were published, but, although the efficiencies significantly increased, especially as concerns organic dye based DSSCs,

Received: January 8, 2013
Accepted: February 28, 2013
Published: February 28, 2013

their values are leveling off (around 12%[2]). As pointed out by Hagfeldt et al.[3] and Snaith et al.,[4] an optimization of these systems should indeed be possible by rationally exploiting their modular structure, associating the different elementary mechanisms to different components. Thus, adequately adjusting the different energetic levels characterizing each chemical component of the cell and also improving the electron transfer between each of them should constitute a viable route of optimization. In this Perspective, it clearly appears how theoretical tools able to provide a deeper understanding of these basic electronic mechanisms, could pave the way to a rational optimization route for these complex devices.

Recently, ab initio approaches based on density functional theory (DFT) and time-dependent DFT (TD-DFT) have proven their ability to model the elementary mechanisms and components of DSSCs.[5−13] The same approaches have thus been used to design and conceive new devices of enhanced properties. The reason for the success of DFT and TD-DFT[14,15] approaches is related to their favorable scaling and cost-to-accuracy ratio, allowing the use of such methods to study both ground and excited state properties of large molecular or periodic systems at the quantum mechanical ab initio level. Nonetheless, some systematic failures of DFT and TD-DFT methods, which may be of relevance for the modeling of DSSCs, are also now well documented in the literature. Among these, the systematic underestimation of the transition energies associated with through-space charge transfer excitations (CT), which are indeed those normally exploited in push−pull dyes used for DSSCs application, when using standard DFT approaches (such as global hybrid functionals), should be taken into account when aiming to design new devices using DFT and TD-DFT based approaches. Analogously, the dramatic underestimation of the gap in semiconductors obtained when using the GGA functional[16−19] should be kept in mind when drawing energetic consideration on dye-semiconductor electronic interactions.

The aim of the present work is to exemplify how the main macroscopic characteristics of a DSSC (such as, for instance, the incident photon-to-charge carrier efficiency (IPCE) curves or J_{SC}) can be properly computed using DFT-based approaches and interpreted in terms of elementary steps when adapted diagnostic theoretical tools[7,20,21] are used in order to define the degree of reliability of the computational approach applied.

The aim of the present work is to exemplify how the main macroscopic characteristic of a DSSC (such as, for instance, the IPCE curves or J_{SC}) can be properly computed using DFT-based approaches and interpreted in terms of elementary steps when adapted diagnostic theoretical tools are used in order to define the degree of reliability of the computational approach applied.

To this end, the performances of three new TiO_2-based DSSCs will be studied, and the results obtained will be compared to the available experimental data. These three devices are characterized by the presence of three donor−acceptor (D−A) push−pull dyes all containing an electron withdrawing moiety belonging to the "expanded pyridinium" family[22,23] (as depicted in Figure 1) differing only for the branched (**B1** and **B2**) or fused (**F1**) architecture of the pyridinium core. In all cases, the electron donor moiety is an amino group: $-NH_2$, in the case of **B1** or **F1**, and $-NMe_2$ for **B2**. The anchoring of the dyes to the semiconductor is achieved by the presence of a carboxylate group.

In order to access some relevant macroscopic characteristics of these three DSSC devices, the following already established[7] stepwise theoretical procedure, based on the use of the same global hybrid functional (PBE0) for DFT and TD-DFT (molecular or periodic) calculations, was adopted:

- Determination of features of the dye by computing its structural and electronic properties;
- Theoretical analysis of the reliability of the computed electronic spectra using density based diagnostic tools;
- Assessment of the impact of adsorption on the dyes' features by determining the electronic structure of a 2D periodic system comprised of a dye molecule and the semiconductor slab;
- Evaluation of the electron injection efficiency, IPCE, and J_{SC}.

Figure 2 reports the experimental absorption spectra along with the related stick spectra obtained at the TD-DFT level (see Supporting Information for experimental and theoretical setup). Overall, at this level of theory,[7,24] an excellent agreement between computed transitions and experimental spectra can be noticed.

All dyes present a single band, associated with a single computed electronic transition, in the visible region, which can be involved in the injection process. In order to assess the nature of this band and confirm the reliability of the computed electronic transition on a fully theoretical basis, especially relevant when the experimental data is not available, an analysis of the transition character exclusively based on the electron density has been performed. The results obtained are reported in Figure 3.

Contrary to the Tozer's index (Λ), analysis of the character of a transition on the basis of the overlap of the module of the orbitals involved,[25] and to its simplified version recently proposed by De Angelis et al. in the framework of DSSCs applications,[10] the index hereafter used (D_{CT}) is based on the variation of the electronic density between a given excited state and the ground state ($\Delta\rho = \rho_{EX} - \rho_{GS}$).[20,21,26] In particular, D_{CT} defines the spatial distance between the two barycenters of the density depletion ($\rho_-(r) = \Delta\rho(r)$ if $\Delta\rho(r) < 0$) and density enhancement ($\rho_+(r) = \Delta\rho(r)$ if $\Delta\rho(r) > 0$) distributions upon excitation.

This approach has some advantages:

- The visualization of $\Delta\rho$ allows the qualitative assignment of the character of the transition. This can avoid a tedious assignment procedure when several monoelectronic excitations contribute to the same electronic transition.
- The distance of charge transfer, D_{CT}, gives a quantitative estimation of the charge transfer length that can help to compare different families of dyes.
- $\Delta\rho$ can be used, also, to compute other fundamental properties of the transition such as the fraction of electron transferred upon transition (q_{CT}), the centroids

dx.doi.org/10.1021/jz400046p | J. Phys. Chem. Lett. 2013, 4, 1044−1050

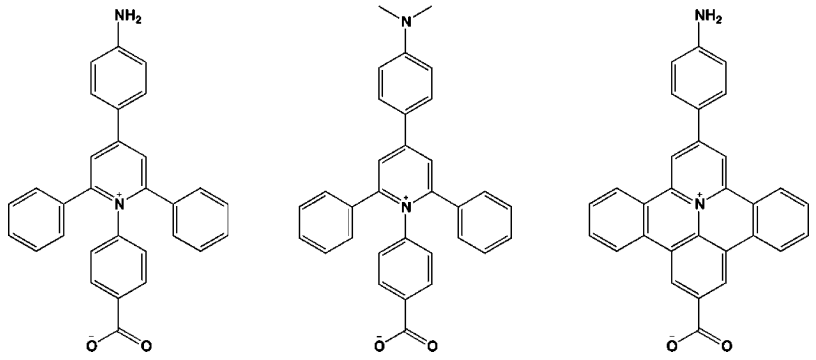

Figure 1. Schematic representation of the **B1** (left), **B2** (middle), and **F1** (right) dyes.

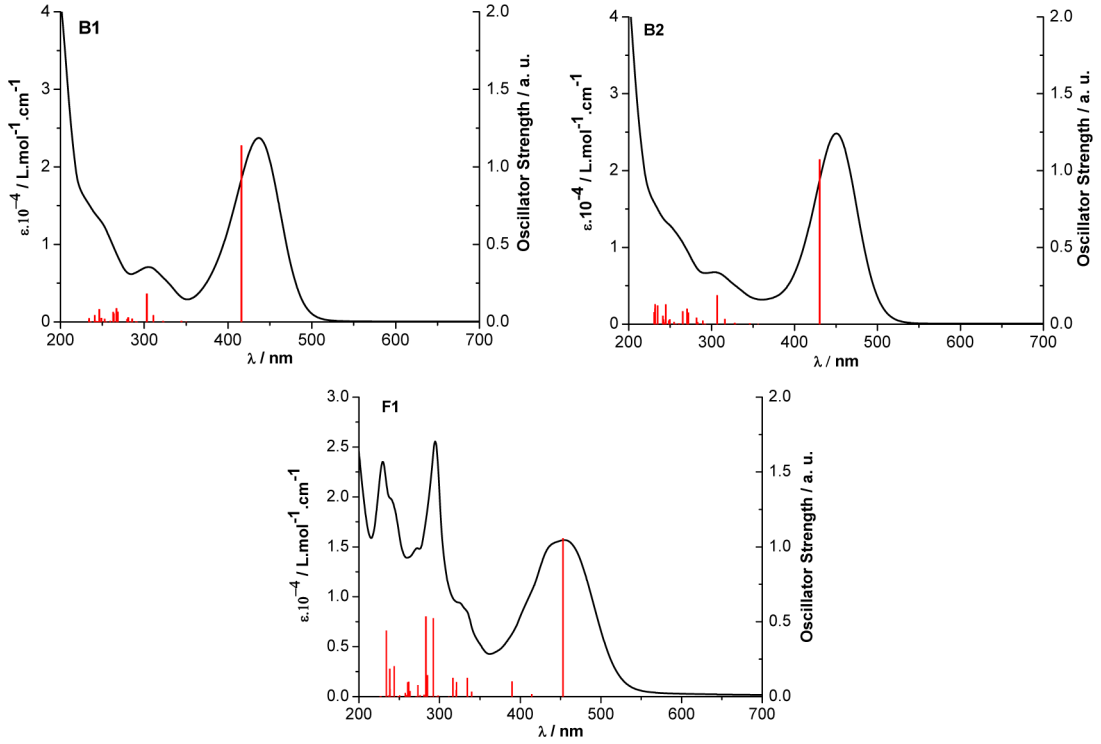

Figure 2. Experimental absorption spectra (black line) along with computed vertical electronic transitions (red bars) of **B1** (top-left), **B2** (top-right), and **F1** (bottom), respectively.

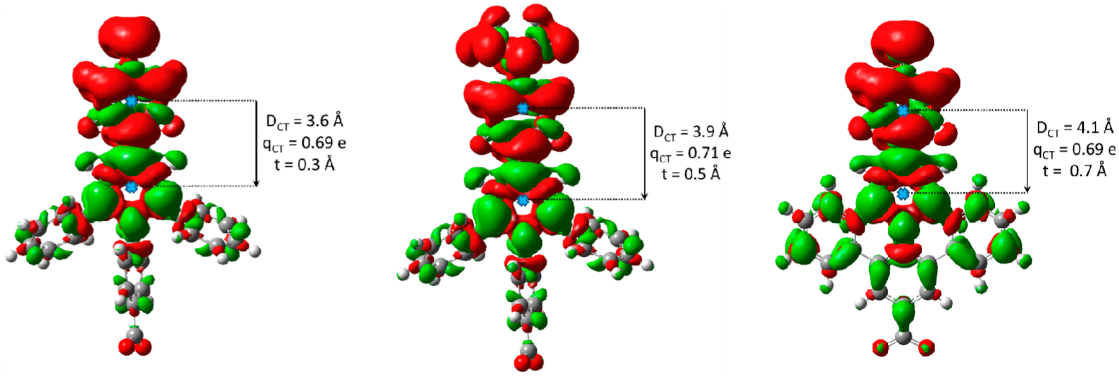

Figure 3. Representations of $\Delta\rho$ (isovalue 0.004 a.u.) associated with the first electronic transition along with the related D_{CT}, q_{CT}, and t indexes computed for **B1**, **B2**, and **F1**, respectively. Green and red zones correspond to positive (ρ_+) and negative (ρ_-) values of $\Delta\rho$, respectively. Barycenters' positions are denoted by blue crosses.

of charge associated to the electronic transition, and a diagnostic index defining the through space CT character of a transition ($t = D_{CT} - H$, H being half of the sum of the centroids axis along electron transfer direction).

dx.doi.org/10.1021/jz400046p | J. Phys. Chem. Lett. 2013, 4, 1044−1050

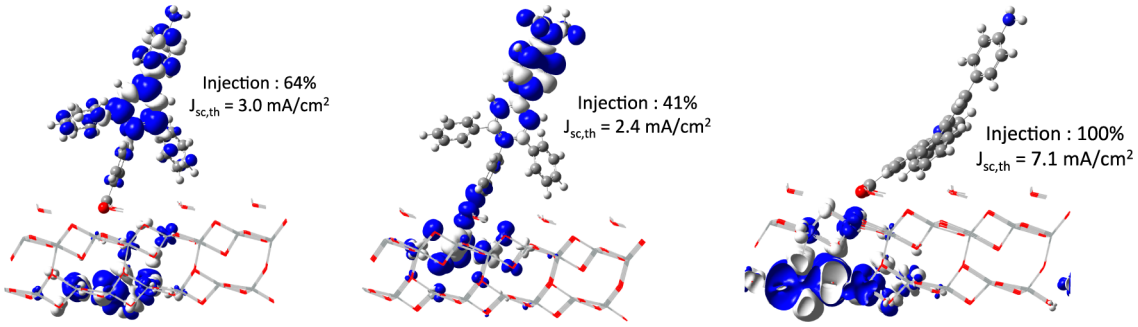

Figure 4. Spin densities of reduced **B1**/TiO_2 (left), **B2**/TiO_2 (middle), and **F1**/TiO_2 (right) systems.

The $\Delta\rho$ associated with the first electronic transition computed for the three dyes is represented in Figure 3. It appears clearly that all these transitions (mainly corresponding to a highest occupied molecular orbital to lowest unoccupied molecular orbital (HOMO−LUMO) excitation) possess a marked charge transfer character, the aminophenyl group acting as electron donor, and the pyridinium moiety behaving as electron acceptor.

The analysis of the D_{CT} index helps in providing quantitative elements of comparison between the different dyes: going from an amino donor (**B1**) to a $-NMe_2$ donor (**B2**) increases the charge transfer length (D_{CT}) by 0.3 Å, while passing from a branched (**B1**) to a fused (**F1**) pyridinium acceptor increases D_{CT} by 0.5 Å.

The computed transferred charge is indeed roughly the same for **B1** and **F1** while slightly larger for **B2**, allowing us to conclude that the strength of the charge transfer (measured by q_{CT}) is more sensitive to the functionalization of the donor group than to the architecture of extended pyridinium core. Nevertheless, the charge transfer length (D_{CT}), of relevance for the use of these systems in DSSC devices, is significantly increased upon polycyclic condensation of the pyridinium core, due to the higher delocalization of the transferred charge possible in the fused architecture (**F1**) than in the branched one (**B1**). Indeed, if the CT character is enhanced by pericondensation of the expanded pyridinium core, the computed t values, all well below the diagnostic threshold of 1.6 Å previously defined in the literature,[20] clearly show that for none of the compounds the transition has a through space character. Thus, the computed t values further confirm the reliability of the computed spectra, beside their agreement with the experimental data.

In order to estimate the main macroscopic characteristic of the device, following a protocol previously applied in the literature, periodic DFT calculations were performed for a system composed by the dye adsorbed on the {101} TiO_2 anatase surface. The free sites of the surface were fully passivated by a water molecule, as previously reported in the literature for a ZnO surface, in order to simulate coadsorption of electrolyte, as a first simple model.[7]

To investigate the electron injection from the dye to the TiO_2 surface (an excited state phenomenon), a computational protocol previously applied to DSSCs,[7,8] relying on the analysis of the corresponding reduced system, was applied. In such a protocol, in analogy to spectroelectrochemistry experiments, the nature of the electronically equilibrated excited state, that is, after the eventual charge injection from the dye to the surface, is modeled by the reduced system.

The localization of the extra-electron in the reduced species is deduced by inspection of the spin density maps, depicted in Figure 4. For the devices containing branched dyes, the extra-electron is localized both on the dye and on the surface, meaning that the injection of the electron is not completely favorable. On the other hand, for the **F1**-based system, a complete electron injection in the TiO_2 slab is predicted, thus underlying that the fusion of the pyridinium core seems to be essential for electron injection, although other isolated dyes characteristics are very similar to branched dyes. The fraction of electron injected is quantified by integrating the spin density on the atoms of the surface: for branched dyes, a fraction of electrons between 0.40 and 0.65 is computed for **B2** and **B1**, respectively, while in the case of **F1**, the electron is computed to be fully injected in the semiconductor.

Once the injection efficiency is computed, the IPCE spectrum of each species is simulated weighting the computed normalized ultraviolet−visible (UV−vis) absorption spectrum, obtained by the computed (TD-DFT) electronic transitions convoluted using the Gaussian function of fixed width (see Supporting Information) for the fraction of injected electron computed by the method presented above. In such a way, theoretical IPCE curves (reported in Figure 5, computational

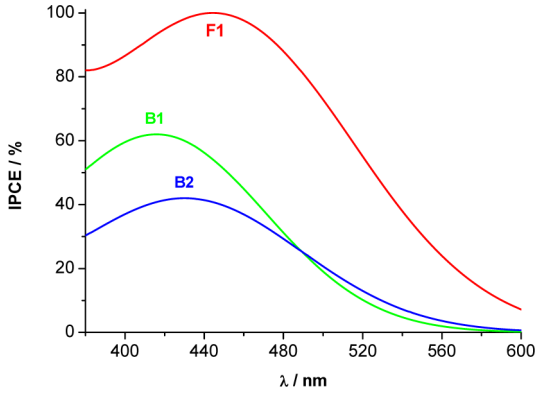

Figure 5. Simulated IPCE curves obtained for **B1** (green), **B2** (blue), and **F1** (red) dyes.

details reported in the Supporting Information) can be obtained. Finally, the theoretical J_{SC} value can be obtained by integration of the computed IPCE spectra as

$$J_{SC} = \frac{hc}{e}\int \lambda \cdot \mathrm{IPCE}(\lambda) \cdot \varphi_{AM1.5}(\lambda)\, d\lambda \quad (6)$$

This protocol, although clearly qualitative, has been previously described in refs 7 and 8 and successfully applied

dx.doi.org/10.1021/jz400046p | J. Phys. Chem. Lett. 2013, 4, 1044−1050

to analyze the influence of the electrolyte composition on the electron injection efficiency. A more quantitative estimate could indeed be obtained applying Marcus theory for a transfer between the excited state of the dye to the conduction band of the semiconductor.

The computed J_{SC} values are reported in Figure 4. The **F1** dye has the highest J_{SC} value, while the **B1** and **B2** dyes show almost the same, and lower, J_{SC}. Indeed, the **B1** higher injection efficiency with respect to **B2** is compensated by a worse overlap of the UV−vis absorption spectrum computed for **B1** with the solar spectrum than in the case of **B2**. For this reason, an almost identical J_{SC} is predicted for **B1** and **B2**.

These theoretical results can be compared to experimental data obtained for TiO_2-based DSSCs sensitized by **B1**, **B2**, and **F1**. The final cell characteristics are presented in Table 1 and in the Supporting Information (together with the experimental setup). The modest efficiencies are principally a consequence of the low V_{oc} (around 0.4 V) measured, which is frequently observed for cationic dyes.[27]

Table 1. Experimental Characteristic Measured for the Different DSSCs

	J_{sc}/mA·cm^{-2}	V_{oc}/V	FF/%	η/%
B1	1.1	0.38	64	0.3
B2	1.2	0.40	67	0.3
F1	5.4	0.39	60	1.3

As theoretically predicted, cells containing the **F1** dyes markedly differ from the ones obtained using branched dyes in term of J_{sc} values. The better performances of F1 are related to the fact that this dye injects more efficiently than branched **B1** and **B2** species. Experimentally, these latter two dyes show almost the same J_{SC} as also predicted by our computational protocol.

Indeed, although the **B2** and **F1** have the same absorption behavior in the visible domain, these dyes provide a completely different efficiency due to their different injection efficiencies.

It seems therefore crucial to setup a computational protocol able to study and optimize not only the properties (i.e., absorption) of the isolated dye but also the properties of the dye-semiconductor interface.

It seems therefore crucial to setup a computational protocol able to study and optimize not only the properties (i.e., absorption) of the isolated dye but also the properties of the dye-semiconductor interface.

DFT- and TD-DFT-based approaches, provided that a functional including a fraction of Hartree−Fock exchange is used, allow nowadays for a good and equilibrated description and prediction of the properties of isolated components and assemblies that constitute the basic elements of DSSCs. In order to avoid spurious effects related to the model used to simulate the semiconductor surface, the so-called confinement effects, a periodic approach seems to be the most reliable to simulate the adsorption of the dye on the surface and the thermodynamically controlled properties of the assemblies.

Using such tools, it is indeed nowadays possible not only to access microscopic quantities but also to global measurable observables such as the IPCE and J_{SC}.

Nonetheless, if current computational approaches have already proven their accuracy for interpretation and design of new cells, it is indeed important to stress that enhancements are still needed, especially to provide a more realistic picture of the kinetic related aspects of the electron injection processes. This latter point is the subject of numerous developments.[11,12,28−36] In particular, a more elaborate description of the elementary electron injection process beside its electronically equilibrated state (currently represented by the reduced system) should be provided in order to fully characterize systems that may be under kinetic control (such as highly flexible ones).

Analogously, the complex structure of the semiconductor−dye interface, here simply modeled by a crystallographic surface saturated by water molecules simulating an electrolyte of complex composition, should be considered as a serious limit when aiming to quantitatively predict the overall characteristic of the device. The influence of electrolyte additive and solvent molecules on the local geometrical and electronic properties of the dye−semiconductor aggregate[7,37−39] as well as of dye−dye interactions[40−42] should explicitly be modeled to obtain a realistic picture of the cell efficiency. Analogously, the dependence of photocurrent density at short-circuit and the open-circuit photovoltage on electron and hole mobility and electron−hole recombination rate should also be included in the model.

Finally, attempts to simulate the electron transfer process involving the redox mediator[43−46] are still at their infancy, although they may play a relevant role in DSSCs' optimization.

■ ASSOCIATED CONTENT

Supporting Information

Computational and experimental setup. This material is available free of charge via the Internet http://pubs.acs.org.

■ AUTHOR INFORMATION

Corresponding Author

*E-mail: tangui.le_bahers@ens-lyon.fr (T.L.B.), carlo-adamo@chimie-paristech.fr (C.A.), Ilaria-ciofini@chimie-paristech.fr (I.C.).

Notes

The authors declare no competing financial interest.

Biographies

Tangui Le Bahers obtained his Ph.D. at Chimie-ParisTech (2011), and now he is an assistant professor between the University of Lyon 1 and the ENS de Lyon (France). He is working on hybrid interfaces involved in artificial photosynthesis (DSSC, water splitting) and in spintronic devices.

Frédéric Labat (Pau, France 1980) graduated and obtained his Ph.D. from Chimie-Paristech (2007). After two years of postdoctoral fellowship (Universite de Pau and Chimie-Paristech, France), he obtained an assistant professor position at Chimie-Paristech (2010). His research interests concern the application of DFT to solid-state systems, with particular emphasis on DSSCs.

Thierry Pauporté received his MS from the ENS de Lyon (France) and his Ph.D from the University Montpellier II (France). He is currently Directeur de recherche at CNRS. His research interests range from the growth of oxides to integration of oxide structures in devices such as solar cell.

Philippe P. Lainé completed his Ph.D. in Toulouse, France in 1993 and, moved to Switzerland for postdoctoral work before returning to Paris as CNRS researcher in 1996. In 2011, he joined the Universite Paris Diderot as CNRS Research Director. He currently works on molecular transduction of energy and information.

Carlo Adamo obtained his Ph.D. from the University of Naples (Italy, 1995). Until 2000 he was Assistant Professor at the University of Basilicata (Italy), and then he moved to Chimie-ParisTech first as an Associate Professor and then as a Full Professor. In 2011 he was admitted to IUF.

Ilaria Ciofini (Arezzo, Italy 1973): MS (Uni. Florence, Italy 1997), Ph.D. (Uni. Fribourg, Switzerland, 2001), one year postdoctoral fellow (Uni.Wurzburg, Germany), two years CNRS associate researcher (Chimie-Paristech). She is currently CNRS Research Director at Chimie-Paristech. Her main research concerns the development and application of DFT methods to molecular compounds.

■ ACKNOWLEDGMENTS

The authors are grateful to the financial help of the bluegene Project No. i2012086883, "Modélisation des cellules photovoltaïques hybrides: effets de l'électrolyte et de la structure de la surface". T.L.B. thanks M. Verot and S. Burema for their fruitful recommendations on graphics design.

■ REFERENCES

(1) O'Regan, B.; Grätzel, M. A Low-Cost, High-Efficiency Solar Cell Based on Dye-Sensitized Colloidal TiO_2 Films. *Nature* **1991**, *353*, 737−740.
(2) Wilson, G.; Boyd, L. http://www.nrel.gov/ncpv/images/efficiency_chart.j, 2012.
(3) Hagfeldt, A.; Boschloo, G.; Sun, L.; Kloo, L.; Pettersson, H. Dye-Sensitized Solar Cells. *Chem. Rev.* **2010**, *110*, 6595−6663.
(4) Snaith, H. J. Estimating the Maximum Attainable Efficiency in Dye-Sensitized Solar Cells. *Adv. Funct. Mater.* **2010**, *20*, 13−19.
(5) Martsinovich, N.; Troisi, A. Theoretical Studies of Dye-Sensitised Solar Cells: from Electronic Structure To Elementary Processes. *Energ. Environ. Sci.* **2011**, *4*, 4473−4495.
(6) Martsinovich, N.; Troisi, A. How TiO_2 Crystallographic Surfaces Influence Charge Injection Rates from a Chemisorbed Dye Sensitiser. *Phys. Chem. Chem. Phys.* **2012**, *14*, 13392−13401.
(7) Le Bahers, T.; Labat, F.; Pauporté, T.; Lainé, P. P.; Ciofini, I. Theoretical Procedure for Optimizing Dye-Sensitized Solar Cells: from Electronic Structure to Photovoltaic Efficiency. *J. Am. Chem. Soc.* **2011**, *133*, 8005−8013.
(8) Labat, F.; Le Bahers, T.; Ciofini, I.; Adamo, C. Insights into Working Principles of Ruthenium Polypyridyl Dye-Sensitized Solar Cells from First Principles Modeling. *Acc. Chem. Res.* **2012**, *45*, 1268−1277.
(9) De Angelis, F.; Fantacci, S.; Selloni, A.; Grätzel, M.; Nazeeruddin, M. K. Influence of the Sensitizer Adsorption Mode on the Open-Circuit Potential of Dye-Sensitized Solar Cells. *Nano Lett.* **2007**, *7*, 3189−3195.
(10) Pastore, M.; Mosconi, E.; Angelis, F. De; Grätzel, M. A Computational Investigation of Organic Dyes for Dye-Sensitized Solar Cells: Benchmark, Strategies, and Open Issues. *J. Phys. Chem. C* **2010**, *114*, 7205−7212.
(11) Persson, P.; Lundqvist, M. J.; Ernstorfer, R.; Goddard, W. a.; Willig, F. Quantum Chemical Calculations of the Influence of Anchor-Cum-Spacer Groups on Femtosecond Electron Transfer Times in Dye-Sensitized Semiconductor Nanocrystals. *J. Chem. Theory Comput.* **2006**, *2*, 441−451.
(12) Jakubikova, E.; Snoeberger, R. C.; Batista, V. S.; Martin, R. L.; Batista, E. R. Interfacial Electron Transfer in TiO_2 Surfaces Sensitized with Ru(II)−Polypyridine Complexes. *J. Phys. Chem. A* **2009**, *113*, 12532−12540.
(13) McNamara, W. R.; Snoeberger, R. C.; Li, G.; Schleicher, J. M.; Cady, C. W.; Poyatos, M.; Schmuttenmaer, C. A.; Crabtree, R. H.; Brudvig, G. W.; Batista, V. S. Acetylacetone Anchors for Robust Functionalization of TiO_2 Nanoparticles with Mn(II)−Terpyridine Complexes. *J. Am. Chem. Soc.* **2008**, *130*, 14329−14338.
(14) Jacquemin, D.; Perpète, E. A.; Ciofini, I.; Adamo, C. Accurate Simulation of Optical Properties in Dyes. *Acc. Chem. Res.* **2009**, *42*, 326−334.
(15) Furche, F.; Ahlrichs, R. Adiabatic Time-Dependent Density Functional Methods for Excited State Properties. *J. Chem. Phys.* **2002**, *117*, 7433.
(16) Labat, F.; Ciofini, I.; Adamo, C. Modeling ZnO Phases Using A Periodic Approach: from Bulk to Surface and Beyond. *J. Chem. Phys.* **2009**, *131*, 044708.
(17) Ahmed, R.; Akbarzadeh, H. A First Principle Study of Band Structure of III-Nitride Compounds. *Physica B* **2005**, *370*, 52−60.
(18) Labat, F.; Baranek, P.; Domain, C.; Minot, C.; Adamo, C. Density Functional Theory Analysis of the Structural and Electronic Properties of TiO_2 Rutile and Anatase Polytypes: Performances of Different Exchange-Correlation Functionals. *J. Chem. Phys.* **2007**, *126*, 154703.
(19) Charifi, Z.; Baaziz, H.; Hussain Reshak, A. Ab-Initio Investigation of Structural, Electronic and Optical Properties for Three Phases of ZnO Compound. *Phys. Status Solidi B* **2007**, *244*, 3154−3167.
(20) Le Bahers, T.; Adamo, C.; Ciofini, I. A Qualitative Index of Spatial Extent in Charge-Transfer Excitations. *J. Chem. Theor. Comput.* **2011**, *7*, 2498−2506.
(21) Ciofini, I.; Le Bahers, T.; Adamo, C.; Odobel, F.; Jacquemin, D. Trough-Space Charge-Transfer in Rod-Like Molecules: Lessons from Theory. *J. Phys. Chem. C* **2012**, *116*, 11946−11955.
(22) Fortage, J.; Peltier, C.; Nastasi, F.; Puntoriero, F.; Tuyèras, F.; Griveau, S.; Bedioui, F.; Adamo, C.; Ciofini, I.; Campagna, S.; Lainé, P. P. Designing Multifunctional Expanded Pyridiniums: Properties of Branched and Fused Head-to-Tail Bipyridiniums. *J. Am. Chem. Soc.* **2010**, *132*, 16700−16713.
(23) Fortage, J.; Tuyèras, F.; Ochsenbein, P.; Puntoriero, F.; Nastasi, F.; Campagna, S.; Griveau, S.; Bedioui, F.; Ciofini, I.; Lainé, P. P. Expanded Pyridiniums: Bis-cyclization of Branched Pyridiniums into Their Fused Polycyclic and Positively Charged Derivatives—Assessing the Impact of Pericondensation on Structural, Electrochemical, Electronic, and Photophysical Features. *Chem.—Eur. J.* **2010**, *16*, 11047−11063.
(24) Le Bahers, T.; Pauporté, T.; Scalmani, G.; Adamo, C.; Ciofini, I. A TD-DFT Investigation of Ground and Excited State Properties in Indoline Dyes used for Dye-Sensitized Solar Cells. *Phys. Chem. Chem. Phys.* **2009**, *11*, 11276−11284.
(25) Peach, M. J. G.; Benfield, P.; Helgaker, T.; Tozer, D. J. Excitation Energies in Density Functional Theory: An Evaluation and a Diagnostic Test. *J. Chem. Phys.* **2008**, *128*, 044118.
(26) Jacquemin, D.; Le Bahers, T.; Adamo, C.; Ciofini, I. What is the "Best" Atomic Charge Model to Describe Through-Space Charge Transfer Excitations? *Phys. Chem. Chem. Phys.* **2012**, *14*, 5383−5388.
(27) Mishra, A.; Fischer, M. K. R.; Bäuerle, P. Metal-Free Organic Dyes for Dye-Sensitized Solar Cells: From Structure:Property Relationships to Design Rules. *Angew. Chem., Int. Ed.* **2009**, *48*, 2474−2499.
(28) Martsinovich, N.; Ambrosio, F.; Troisi, A. Adsorption and Electron Injection of the N3 Metal−Organic Dye on the TiO_2 Rutile
(110) Surface. *Phys. Chem. Chem. Phys.* **2012**, *14*, 16668−16676.
(29) Jones, D. R.; Troisi, A. A Method to Rapidly Predict the Charge Injection Rate in Dye Sensitized Solar Cells. *Phys. Chem. Chem. Phys.* **2010**, *12*, 4625−34.
(30) Jiao, Y.; Ding, Z.; Meng, S. Atomistic Mechanism of Charge Separation upon Photoexcitation at the Dye−Semiconductor Interface for Photovoltaic Applications. *Phys. Chem. Chem. Phys.* **2011**, *13*, 13196−13201.

(31) Martsinovich, N.; Troisi, A. High-Throughput Computational Screening of Chromophores for Dye-Sensitized Solar Cells. *J. Phys. Chem. C* **2011**, *115*, 11781−11792.
(32) Maggio, E.; Martsinovich, N.; Troisi, A. Evaluating Charge Recombination Rate in Dye-Sensitized Solar Cells from Electronic Structure Calculations. *J. Phys. Chem. C* **2012**, *116*, 7638−7649.
(33) Kondov, I.; Cizek, M.; Benesch, C.; Wang, H.; Thoss, M. Quantum Dynamics of Photoinduced Electron-Transfer Reactions in Dye−Semiconductor Systems: First-Principles Description and Application to Coumarin 343−TiO_2. *J. Phys. Chem. C* **2007**, *111*, 11970−11981.
(34) Abuabara, S. G.; Cady, C. W.; Baxter, J. B.; Schmuttenmaer, C. A.; Crabtree, R. H.; Brudvig, G. W.; Batista, V. S. Ultrafast Photooxidation of Mn(II)−Terpyridine Complexes Covalently Attached to TiO_2 Nanoparticles. *J. Phys. Chem. C* **2007**, *111*, 11982−11990.
(35) Rego, L. G. C.; Silva, R.; Freire, A.; Snoeberger, R. C.; Batista, V. S. Visible Light Sensitization of TiO_2 Surfaces with Alq3 Complexes. *J. Phys. Chem. C* **2010**, *114*, 1317−1325.
(36) McNamara, W. R.; Snoeberger, R. C., III; Li, G.; Richter, C.; Allen, L. J.; Milot, R. L.; Schmuttenmaer, C. a.; Crabtree, R. H.; Brudvig, G. W.; Batista, V. S. Hydroxamate Anchors for Water-Stable Attachment to TiO_2 Nanoparticles. *Energ. Environ. Sci.* **2009**, *2*, 1173−1175.
(37) Le Bahers, T.; Labat, F.; Pauporté, T.; Ciofini, I. Solvent and Additives Effects on the Open Circuit Voltage of ZnO Based Dye-Sensitized-Solar Cells: A Combined Theoretical and Experimental Study. *Phys. Chem. Chem. Phys.* **2010**, *12*, 14710−14719.
(38) De Angelis, F.; Fantacci, S.; Gebauer, R. Simulating Dye-Sensitized TiO_2 Heterointerfaces in Explicit Solvent: Absorption Spectra, Energy Levels, and Dye Desorption. *J. Phys. Chem. Lett.* **2011**, *2*, 813−817.
(39) Kusama, H.; Orita, H.; Sugihara, H. TiO_2 Band Shift by Nitrogen-Containing Heterocycles in Dye-Sensitized Solar Cells: A Periodic Density Functional Theory Study. *Langmuir* **2008**, *24*, 4411−4419.
(40) Pastore, M.; De Angelis, F. Aggregation of Organic Dyes on TiO_2 in Dye-Sensitized Solar Cells Models: An ab Initio Investigation. *ACS Nano* **2010**, *4*, 557−562.
(41) Pastore, M.; De Angelis, F. First-Principles Computational Modeling of Fluorescence Resonance Energy Transfer in Co-Sensitized Dye Solar Cells. *J. Phys. Chem. Lett.* **2012**, *3*, 2146−2153.
(42) Kusama, H.; Sayama, K. Theoretical Study on the Intermolecular Interactions of Black Dye Dimers and Black Dye−Deoxycholic Acid Complexes in Dye-Sensitized Solar Cells. *J. Phys. Chem. C* **2012**, *116*, 23906−23914.
(43) Kusama, H.; Sugihara, H.; Sayama, K. Effect of Cations on the Interactions of Ru Dye and Iodides in Dye-Sensitized Solar Cells: A Density Functional Theory Study. *J. Phys. Chem. C* **2010**, *115*, 2544−2552.
(44) Kusama, H.; Sugihara, H.; Sayama, K. Simultaneous Interactions of Ru Dye with Iodide Ions and Nitrogen-Containing Heterocycles in Dye-Sensitized Solar Cells. *J. Phys. Chem. C* **2010**, *114*, 11335−11341.
(45) Pastore, M.; Mosconi, E.; De Angelis, F. Computational Investigation of Dye−Iodine Interactions in Organic Dye-Sensitized Solar Cells. *J. Phys. Chem. C* **2012**, *116*, 5965−5973.
(46) Hu, C-H; Asaduzzaman, A. M.; Schreckenbach, G. Computational Studies of the Interaction between Ruthenium Dyes and X^- and X_2^-, X = Br, I, At. Implications for Dye-Sensitized Solar Cells. *J. Phys. Chem. C* **2010**, *114*, 15165−15173.